NANO LETTERS

Letter

pubs.acs.org/NanoLett

Axon-First Neuritogenesis on Vertical Nanowires

Kyungtae Kang,[†,‡] Yi-Seul Park,[§] Matthew Park,[†] Min Jee Jang,[‡] Seong-Min Kim,[∥] Juno Lee,[†] Ji Yu Choi,[†] Da Hee Jung,[§] Young-Tae Chang,[⊥] Myung-Han Yoon,[*,∥] Jin Seok Lee,[*,§] Yoonkey Nam,[*,‡] and Insung S. Choi[*,†,‡]

[†]Center for Cell-Encapsulation Research and Molecular-Level Interface Research Center, Department of Chemistry, KAIST, Daejeon 34141, Korea

[‡]Department of Bio and Brain Engineering, KAIST, Daejeon 34141, Korea

[§]Department of Chemistry, Sookmyung Women's University, Seoul 04310, Korea

[∥]School of Materials Science and Engineering, Gwangju Institute of Science and Technology, Gwangju 61005, Korea

[⊥]Department of Chemistry, National University of Singapore, Singapore 117543, Singapore

Supporting Information

ABSTRACT: In this work, we report that high-density, vertically grown silicon nanowires (*vg*-SiNWs) direct a new *in vitro* developmental pathway of primary hippocampal neurons. Neurons on *vg*-SiNWs formed a single, extremely elongated major neurite earlier than minor neurites, which led to accelerated polarization. Additionally, the development of lamellipodia, which generally occurs on 2D culture coverslips, was absent on *vg*-SiNWs. The results indicate that surface topography is an important factor that influences neuronal development and also provide implications for the role of topography in neuronal development *in vivo*.

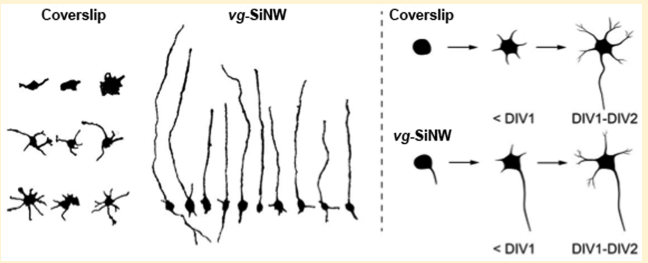

KEYWORDS: *Silicon nanowires, neurite development, F-actin dynamics, primary hippocampal neuron, chemical vapor deposition, live-cell imaging*

Recent reports showed that surface topography, particularly at the nanoscale, determined the rate of early *in vitro* neurite development. Nanostructured surfaces (silica-bead monolayers,[1,2] anodized aluminum oxide,[3] and electrospun fibers[4,5]) accelerated neurite outgrowth and the polarization of neurons, compared with flat culture plates. For example, electrospun nanofibers accelerated neuritogenesis, the initial formation of neurites, of primary motor neurons, but did not affect the average length of their neurites, when compared with flat, glass coverslips.[4,5] However, hippocampal neurons cultured on anodized aluminum oxide and silica-bead monolayers showed accelerated development and neurite elongation depending on the pitch of nanostructures, with a threshold of ~200 nm.[1,3] Further biochemical study of this nanotopographical effect on neurite development revealed that actin dynamics, the dynamic activities (e.g., protrusion/retraction and turning) of the two actin-based cytoplasmic projections (lamellipodia and filopodia), were engaged in the recognition of the nanotopographical environment and the resultant developmental acceleration.[2] These findings suggested the presence of intraneuronal machinery that can elicit developmental changes in response to surface nanotopography.

Vertically grown nanowires, in addition to being utilized as intra/extracellular electrodes,[6−8] probes to measure cellular forces,[9] or vehicles for the delivery of biomolecules,[10] have also served as nanotopographical substrates to elicit a wide variety of interesting neuronal behaviors and developmental changes, including enhanced adhesion and directionally guided neurite outgrowth.[12−14] For example, Hällstrom et al. reported that vertically grown gallium phosphide nanowires supported neuronal adhesion and survival without adhesive chemical coatings, and they subsequently used the structures for guiding axonal growth.[11,12] Another approach utilized platinum nanopillar arrays for physically restricting the migration of neurons.[13] More recently, Bugnicourt et al. reported the developmental acceleration of primary neurons on ion-etched shallow Si nanopillars.[14]

Despite the various documented effects of nanotopography on neuronal development, however, neurons in these studies still followed the previously known progression of *in vitro* neuronal development:[15] (i) cell spreading and formation of lamellipodia; (ii) formation of multiple, indistinguishable neurites; (iii) elongation of a single, major neurite (which often develops into an axon). Thus, the determination of the major neurite resulted from a "tug of war" between the preformed neurites. There have been, however, no reports on

Received: November 2, 2015
Revised: December 7, 2015
Published: December 8, 2015

DOI: 10.1021/acs.nanolett.5b04458
Nano Lett. 2016, 16, 675−680

changes in the mechanism of the determination of a major neurite; more specifically, the major neurite rapidly elongates (*stage iii*) before forming multiple minor neurites (*stage ii*), which might have a higher relevance to the neuronal development that occurs in brains.[16−18] In this work, we used a discontinuous, semi-3D structure of vertically grown silicon nanowires (*vg*-SiNWs) as a culture platform and found that primary hippocampal neurons bypassed the initial formation of multiple neurites and instead exhibited a permutated progression of neuronal development, deviating from the previously shown *in vitro* developmental stages.

Hippocampal neurons derived from E18 Sprague−Dawley rat were plated at a density of 100−200 cells/mm^2 and cultured on *vg*-SiNW substrates (diameter, 72 ± 8 nm; length, 7 to 10 μm; density, 17.9 NW/μm^2; see the Supporting Information for the synthesis and characteristics of *vg*-SiNWs). Even at 1 day *in vitro* (DIV), the neuronal morphologies observed on *vg*-SiNWs did not belong to any conventional developmental stages observed on coverslips. The majority of the neurons on *vg*-SiNWs were already highly polarized with one extensively elongated major neurite and possessed few minor neurites (no or 1 minor neurite in some cases) (Figure 1), which indicated

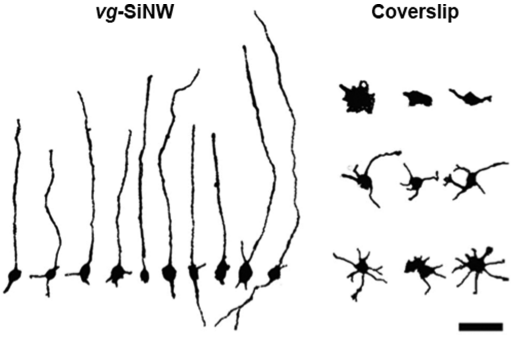

Figure 1. Neurites develop differently on *vg*-SiNWs. Drawings taken from photomicrographs (at 1 DIV) of neurons on *vg*-SiNWs (left) and coverslips (right). The scale bar is 30 μm.

that a major neurite (i.e., axon) was determined before multiple minor neurites formed, as opposed to the simultaneous formation observed on coverslips (Supplementary Movie). The average length of the longest neurite was 4-fold longer on *vg*-SiNWs than coverslips (Figure 2a). An analysis of the numbers of neurites further supported the difference in neuritogenesis. When compared with neurons at 1 DIV, the number of neurons containing two neurites was significantly higher for neurons grown on *vg*-SiNWs (37% of the total samples vs 15% for 1 DIV; Figure 2b), and the number of neurons containing zero neurites was significantly lower (15% of the total neurons vs 30% for 1 DIV). Notably, more than half (~60%) of neurons on *vg*-SiNWs had 1 or 2 neurites, resulting in a narrower range of the numbers of neurites. In addition to the morphological differences, another striking contrast arose in their contact with the surfaces. The scanning electron microscopy (SEM) images showed that the cell body (soma) was supported by *vg*-SiNWs, resulting in the discontinuous interactions with only the upper regions of the *vg*-SiNWs (Figure 2c), whereas neurons on flat coverslips were generally observed to be spread well with lamellipodia. The tips of neurites on a *vg*-SiNW tended to grasp a proximal *vg*-SiNW and jumped through the gap between the *vg*-SiNWs. These grasping

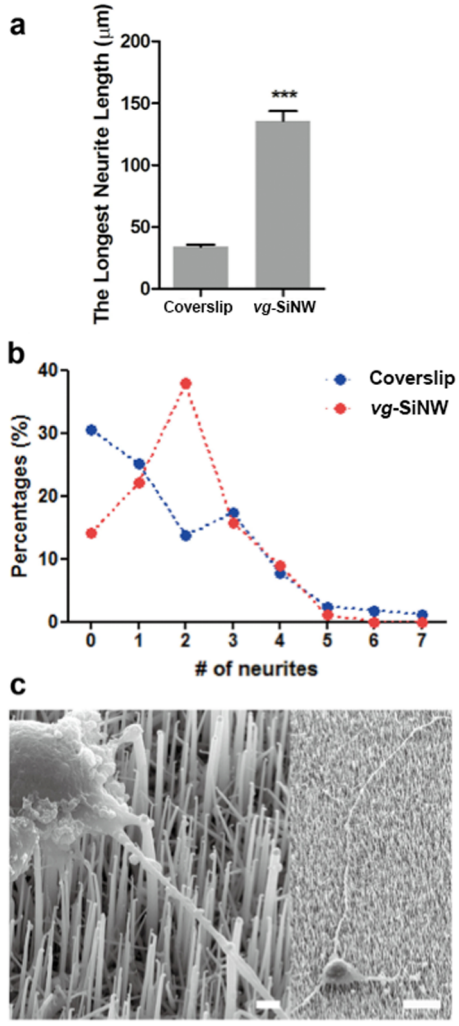

Figure 2. (a) Average lengths (mean ± S.E.) of the longest neurites at 1 DIV. ***P < 0.001. The neurons without neurites were excluded from the analysis. (b) Detailed populations of neurons with each number of neurites on *vg*-SiNWs and coverslips. (c) SEM micrographs of hippocampal neurons cultured on *vg*-SiNWs. The images were taken with the cells fixed at 1 DIV, and the scale bars are 2 and 30 μm for the left and right images, respectively.

behaviors were observed more frequently for the thicker *vg*-SiNWs.

Detailed observation of neurite development for the initial 12 h showed that the polarization of a neuron (formation and elongation of a major neurite) on *vg*-SiNWs occurred, surprisingly, at 3 h *in vitro* at least. Other morphological changes, such as dendritic outgrowth, were not seen during the initial 12 h of culture (Figure 3a). The average rate of the elongation was measured to be 3.96 μm/h, which was much faster than that on a coverslip at 1.5 DIV, when a major neurite was decided out of minor neurites (1.86 μm/h, Figure 3b). That is, the *vg*-SiNWs accelerated both neuritogenesis and neurite outgrowth. The analysis of the number of neurites further consolidated the observed developmental differences in the initial 12 h of growth (Figure 3c). On coverslips, the average number of neurites per neuron was fairly low and did not increase throughout the initial period (at 3 h *in vitro*: 0.5 ± 0.13, n = 38, mean ± S.E.), but increased abruptly between 12 and 24 h *in vitro* (from 0.28 ± 0.16 to 1.67 ± 0.13, n = 18 and 167, respectively). The sudden surge reflected that the

DOI: 10.1021/acs.nanolett.5b04458
Nano Lett. 2016, 16, 675−680

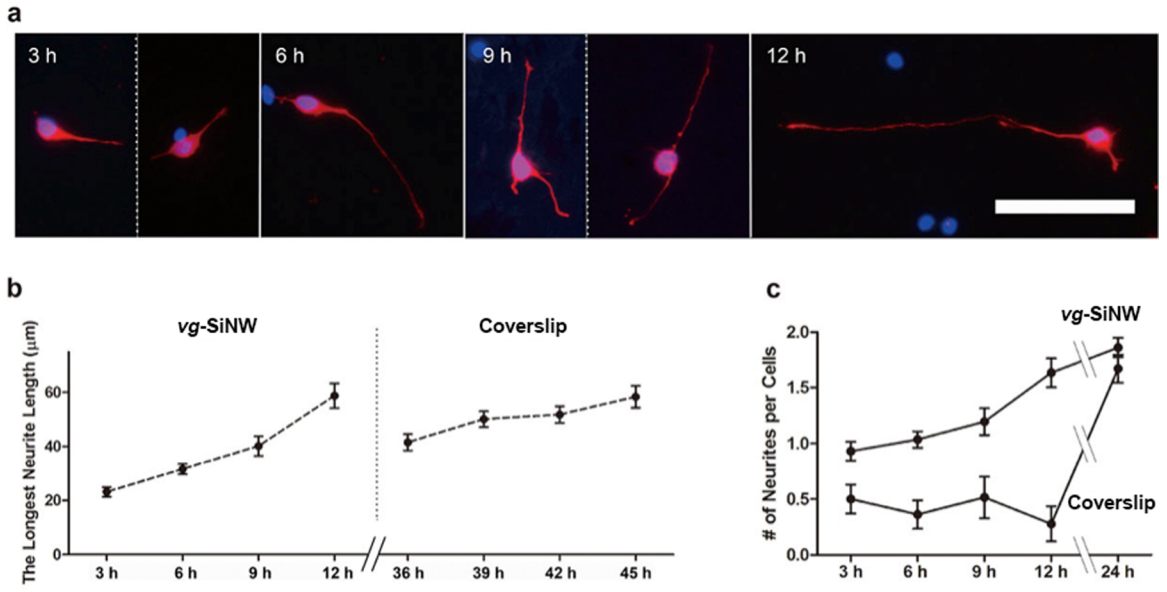

Figure 3. Neuritogenesis occurs extremely early on *vg*-SiNWs. (a) Neurite development on *vg*-SiNWs earlier than 1 DIV (3−12 h) shown by immunostaining *β*-tubulin-III. The scale bar is 50 *μ*m. (b) Average lengths of the longest neurites (mean ± S.E.) on *vg*-SiNWs and coverslips, periodically measured from the time of major neurite designation/formation (immediately and 36 h after plating for *vg*-SiNWs and coverslips, respectively). (c) The numbers of neurite per neurons (mean ± S.E.) within 1 day on *vg*-SiNWs and coverslips.

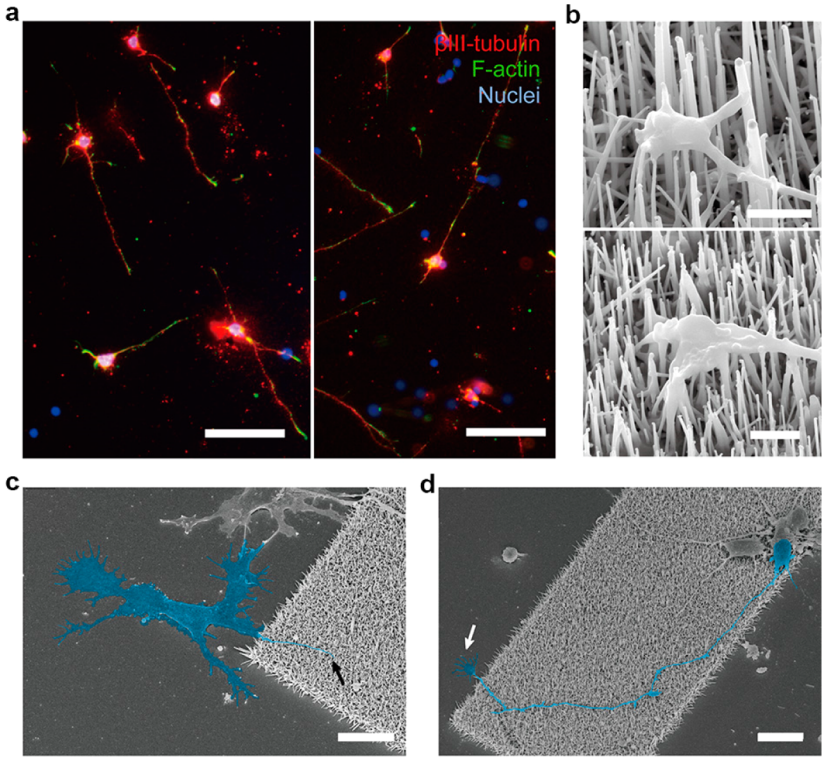

Figure 4. Neurites on *vg*-SiNWs do not contain growth cone structures. (a) Immunostained hippocampal neurons on *vg*-SiNWs (1 DIV). Target: *β*-tubulin-III (red), F-actin (green). The scale bars are 50 *μ*m. (b) SEM micrographs of two representative tip structures of the neurites on *vg*-SiNWs. The scale bars are 2 *μ*m. (c,d) SEM micrographs of neurons on patterned *vg*-SiNWs. Line patterns (width: 50 *μ*m) of *vg*-SiNWs were obtained by using Si(111) substrates with patterned Au films. Both bare and *vg*-SiNW regions were amine-coated. The black and white arrows denote the tip structures of neurites from the false-colored neurons on *vg*-SiNW (black) and flat (white) surfaces. (c) Neurite on the *vg*-SiNW region, sprouted from a soma off the *vg*-SiNW region, and vice versa for (d). The scale bars are 12 *μ*m.

formation of multiple minor neurites occurred intensively during this period. In contrast, the number of neurites on *vg*-SiNWs increased gradually, without a drastic increase, while starting with more neurites than neurons on coverslips (from 0.93 ± 0.08 at 3 h *in vitro* to 1.87 ± 0.09 at 24 h *in vitro*; $n = 72$ and 190, respectively). These different progressions of neurite development suggested that the polarization of the neurons on

DOI: 10.1021/acs.nanolett.5b04458
Nano Lett. 2016, 16, 675−680

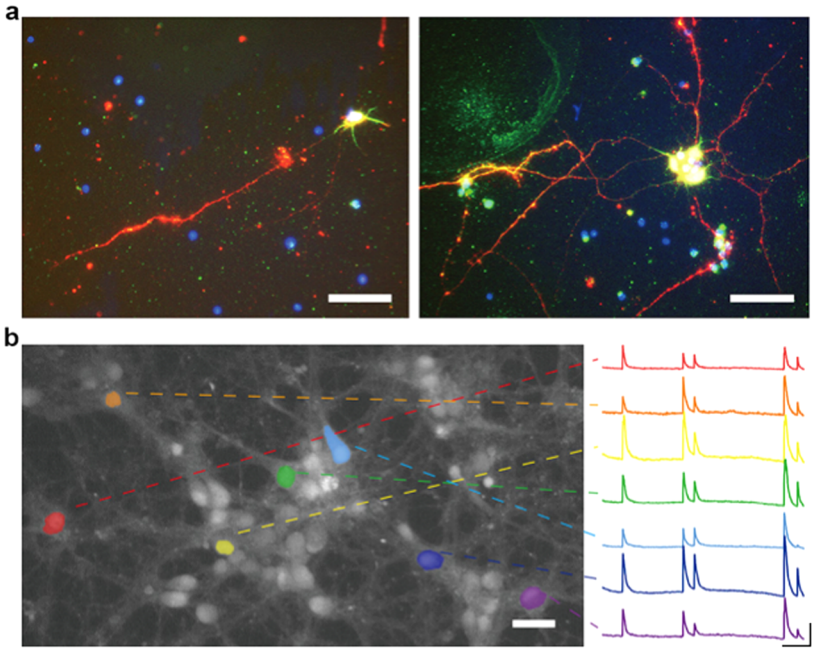

Figure 5. Hippocampal neurons on *vg*-SiNWs develop functional inner structures eventually. (a) Two representative images of hippocampal neurons on *vg*-SiNWs (5 DIV) immunostained with anti-tau (red) for axons and anti-MAP2 (green) for dendrites, showing development of axons and dendrites. (b) *In vitro* somatic calcium imaging from hippocampal neurons at 11 DIV on *vg*-SiNWs. Left, a fluorescence micrograph of the neurons after loading of Oregon Green Bapta-1. The scale bar is 30 μm. Right, relative changes in fluorescence ($\Delta F/F$) of the seven representative neurons in the left image. Spontaneous activity of neurons was induced by adding 5 mM of KCl to the bath solution. The somata of neurons (left) were marked as 7 different colors, each of which matches that of the corresponding calcium signal trace (right). The scale bars are 10% $\Delta F/F$ and 10 s.

vg-SiNWs was not simply faster, but rather was a manifestation of a completely different developmental pathway.

In order to further observe the intracellular activity of neurons on *vg*-SiNWs, we labeled F-actin structures using immunocytochemistry. As shown in Figure 4a, the neurons on *vg*-SiNWs did not significantly develop protruded F-actin structures (i.e., lamellipodia and filopodia), but instead F-actin was colocalized with microtubules. At an earlier stage (3 h *in vitro*), the neurons without neurites had F-actin accumulated at one specific site of the somata, which later became the initiation site for subsequent neuritogenesis (Figure S4). This directional accumulation of F-actin was previously reported on another nanotopographical surface[15] and indicates that there may be a different way by which F-actin dynamics are interpreted by neurons on nanotopographies from conventional 2D surfaces. The magnified SEM images of the neurite tips also showed none or more shrunken structures of growth cone, compared with what were observed on coverslips. Without lamellipodia nor filopodia, some of the tips of neurites contained several tiny processes grasping the adjacent nanowires (Figure 4b). Nonetheless, the shrinkage or absence of growth cones was not a dead-end phenomenon, as their formation was fully restored when the neurites faced flat surfaces. When we cultured neurons on a line-patterned *vg*-SiNW substrate, the neurons on flat regions showed lamellipodial development and growth cone formation, and those on *vg*-SiNWs did not, consistent with the data on *vg*-SiNW only. However, the neurons spanning both regions showed both types of the neurite development, depending upon the location of neurite tips (Figure 4c,d). The neurite did not possess normal F-actin protrusions on *vg*-SiNWs even when it sprouted from the soma that lied on a flat region. Conversely, neurites sprouting from the soma on *vg*-SiNWs developed the growth cone structures with filopodia, if they were on flat regions. The results indicated that the *vg*-SiNWs did not irreversibly induce cellular-level changes in neurons, and the morphological changes were contact-based.

Despite striking differences in the initial development, the neurons on *vg*-SiNWs matured and formed a functional neuronal network as those on coverslips. At 5 DIV the neurons expressed tau (axon-specific protein) and microtubule-associated protein 2 (MAP2, dendrite-specific protein) in a localized manner (Figure 5a). The structural intactness of neurites (axons and dendrites) indicated that the *vg*-SiNW nanotopography did not impair the neuronal development, but only altered the neuritogenesis process. At 11 DIV, the somata tended to aggregate, and the neurites were developed extensively and almost covered the entire *vg*-SiNW substrate. The somatic calcium signals measured from the selected neurons at 11 DIV showed that most of the spontaneous calcium spikes were synchronized, implying the presence of funtional connections between the neurons (Figure 5b).

In the homogeneous, uniform environment of 2D culture plates, the determination of an axon among neurites depends on a "tug of war" between the neurites,[19,20] but these *in vitro* cytoskeletal dynamics of the two actin-based projections do not fully recapitulate *in vivo* neuronal development,[21−23] as exemplified by the development of neuroblasts,[16] neurons in zebrafish optic tectum,[17] and retinal ganglion axons.[18] Most neurons in these cases develop a single neurite, which becomes an axon later, first, followed by multiple neurites at the later stages. Although the morphology or stiffness of *vg*-SiNWs are dissimilar to the soft environments in brains, the finding of the new *in vitro* developmental pathway of hippocampal neurons on *vg*-SiNWs (Figure 6a, constructed from the results) suggests that the developmental differences between *in vivo* and *in vitro* neurons might arise, at least partially, from the topography of the surfaces that the neurons encounter. The earlier develop-

DOI: 10.1021/acs.nanolett.5b04458
Nano Lett. 2016, 16, 675−680

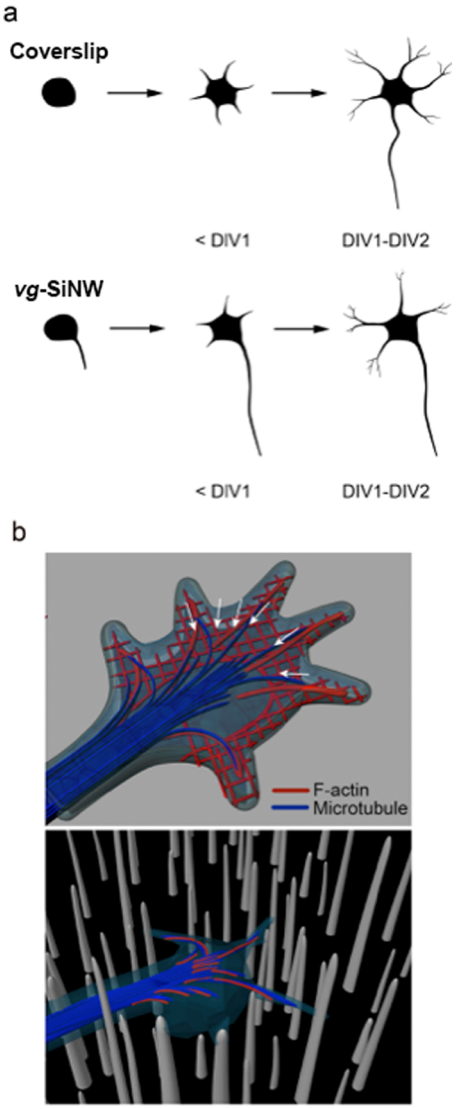

Figure 6. Nanotopography of *vg*-SiNWs induces a different developmental pathway for hippocampal neurons. (a) Illustrations of the representative morphologies of hippocampal neurons at their initial developmental stages on coverslips and *vg*-SiNW surfaces. (b) Microtubules and F-actin structures at the tips of the neurons on flat and *vg*-SiNW surfaces. White arrows denote the regulation of advances of microtubules, exerted by F-actin fibers.

ment of a remarkably long, single neurite and the impeded formation of F-actin structures, which we observed on *vg*-SiNWs but not on coverslips, are quite reminiscent, albeit only morphologically, so far, of what occurs *in vivo*. The results also imply that the different developmental pathway might be caused by changes in dynamic formation/deformation of F-actin structures, as an inhibitory regulator for the advance of microtubule fibers (Figure 6b). However, the specific features of *vg*-SiNWs that induce a different developmental pathway in neurons, other than just accelerate their development, still remain uncertain. Future efforts should focus on (i) searching the exact features of the surface nanotopographies that can alter the developmental pathway of neurons, and (ii) the proteomic and transcriptomic comparisons of the neurons cultured on such nanotoporgaphies with those cultured *in vivo*. We believe that the finding of the current work will significantly contribute to our knowledge of the developmental biology of neurons by encouraging synergistic interactions between the fields of nanoscience, biochemistry, and cell biology.

■ ASSOCIATED CONTENT

Supporting Information

The Supporting Information is available free of charge on the ACS Publications website at DOI: 10.1021/acs.nanolett.5b04458.

Further details on cell culture and imaging procedures, as well as additional information on *vg*-SiNW fabrication and analysis (PDF)

Neurons on coverslips and *vg*-SiNWs (AVI)

■ AUTHOR INFORMATION

Corresponding Authors

*E-mail: ischoi@kaist.ac.kr.
*E-mail: ynam@kaist.ac.kr.
*E-mail: jinslee@sookmyung.ac.kr.
*E-mail: myoon@gist.ac.kr.

Author Contributions

K.K., Y.-S.P., and M.P. contributed equally to this work. K.K., J.S.L., Y.N., and I.S.C. conceived and designed the experiments. K.K., M.P., and J.Y.C. performed the biological experiments. Y.-S.P., D.H.J., and J.S.L. fabricated the substrates. M.J.J., S.-M.K., M.-H.Y., and Y.N. conducted the time-lapse imaging analysis and the calcium imaging analysis. J.L. contributed graphical works. Y.T.C. provided NeuO for imaging. K.K., Y.-S.P., M.P., J.S.L., Y.N., and I.S.C. cowrote the paper. All authors commented the paper.

Notes

The authors declare no competing financial interest.

■ ACKNOWLEDGMENTS

This work was supported by the Basic Science Research Program through the National Research Foundation of Korea funded by Ministry of Science, ICT, and Future Planning (2012R1A3A2026403 and 2015R1A2A1A09003605, 2015R1A2A2A01005556, 2012M3A7B4034986, 2012-0009562, and 20090083525). The authors thank Neural Engineering Laboratory members for assisting cell culture experiments and providing valuable inputs.

■ REFERENCES

(1) Kang, K.; Choi, S. E.; Jang, H. S.; Cho, W. K.; Nam, Y.; Choi, I. S.; Lee, J. S. *Angew. Chem., Int. Ed.* **2012**, *51*, 2855.
(2) Kang, K.; Yoon, S. Y.; Choi, S. E.; Kim, M.-H.; Park, M.; Nam, Y.; Lee, J. S.; Choi, I. S. *Angew. Chem., Int. Ed.* **2014**, *53*, 6075.
(3) Cho, W. K.; Kang, K.; Kang, G.; Jang, M. J.; Nam, Y.; Choi, I. S. *Angew. Chem., Int. Ed.* **2010**, *49*, 10114.
(4) Gertz, C. C.; Leach, M. K.; Birrell, L. K.; Martin, D. C.; Feldman, E. L.; Corey, J. M. *Dev. Neurobiol.* **2010**, *70*, 589.
(5) Xie, J.; MacEwan, M. R.; Li, X.; Sakiyama-Elbert, S. E.; Xia, Y. *ACS Nano* **2009**, *3*, 1151.
(6) Patolsky, F.; Timko, B. P.; Yu, G.; Fang, Y.; Greytak, A. B.; Zheng, G.; Lieber, C. M. *Science* **2006**, *313*, 1100.
(7) Robinson, J. T.; Jorgolli, M.; Shalek, A. K.; Yoon, M.-H.; Gertner, R. S.; Park, H. *Nat. Nanotechnol.* **2012**, *7*, 180.
(8) Cohen-Karni, T.; Qing, Q.; Li, Q.; Fang, Y.; Lieber, C. M. *Nano Lett.* **2010**, *10*, 1098.
(9) Hallstrom, W.; Lexholm, M.; Suyatin, D. B.; Hammarin, G.; Hessman, D.; Samuelson, L.; Montelius, L.; Kanje, M.; Prinz, C. N. *Nano Lett.* **2010**, *10*, 782.

DOI: 10.1021/acs.nanolett.5b04458
Nano Lett. 2016, 16, 675−680

(10) Shalek, A. K.; Robinson, J. T.; Karp, E. S.; Lee, J. S.; Ahn, D. R.; Yoon, M.-H.; Sutton, A.; Jorgolli, M.; Gertner, R. S.; Gujral, T. S.; MacBeath, G.; Yang, E. G.; Park, H. *Proc. Natl. Acad. Sci. U. S. A.* **2010**, *107*, 1870.
(11) Hallstrom, W.; Martensson, T.; Prinz, C.; Gustavsson, P.; Montelius, L.; Samuelson, L.; Kanje, M. *Nano Lett.* **2007**, *7*, 2960.
(12) Prinz, C.; Hallstrom, W.; Martensson, T.; Samuelson, L.; Montelius, L.; Kanje, M. *Nanotechnology* **2008**, *19*, 345101.
(13) Xie, C.; Hanson, L.; Xie, W.; Lin, Z.; Cui, B.; Cui, Y. *Nano Lett.* **2010**, *10*, 4020.
(14) Bugnicourt, G.; Brocard, J.; Nicolas, A.; Villard, C. *Langmuir* **2014**, *30*, 4441.
(15) Dotti, C. G.; Sullivan, C. A.; Banker, G. A. *J. Neurosci.* **1988**, *8*, 1454.
(16) da Silva, J. S.; Dotti, C. G. *Nat. Rev. Neurosci.* **2002**, *3*, 694.
(17) Kaethner, R. J.; Stuermer, C. A. *J. Neurobiol.* **1997**, *32*, 627.
(18) Bovolenta, P.; Mason, C. *J. Neurosci.* **1987**, *7*, 1447.
(19) Witte, H.; Bradke, F. *Curr. Opin. Neurobiol.* **2008**, *18*, 479.
(20) Craig, A. M.; Banker, G. *Annu. Rev. Neurosci.* **1994**, *17*, 267.
(21) Huang, J.; Grater, S. V.; Corbellini, F.; Rinck, S.; Bock, E.; Kemkemer, R.; Kessler, H.; Ding, J.; Spatz, J. P. *Nano Lett.* **2009**, *9*, 1111.
(22) Graeter, S. V.; Huang, J.; Perschmann, N.; Lopez-Garcia, M.; Kessler, H.; Ding, J.; Spatz, J. P. *Nano Lett.* **2007**, *7*, 1413.
(23) Liu, Y.; Medda, R.; Liu, Z.; Galior, K.; Yehl, K.; Spatz, J. P.; Cavalcanti-Adam, E. A.; Salaita, K. *Nano Lett.* **2014**, *14*, 5539.

DOI: 10.1021/acs.nanolett.5b04458
Nano Lett. 2016, 16, 675−680